Chapter 6

The plausible correlation between b-value and radon gas anomalies

Chapter 6

The plausible correlation between b-value and radon gas anomalies

6.1. Introduction

Numerous investigations have explored phenomena preceding earthquakes, including magnetic and electric fields, gas emissions, changes in groundwater level, temperature fluctuations, ground fractures, and seismic activity. The temporal decrease in b-value and radon gas anomalies well before major events are also considered among the most well-proven earthquake precursors. In the quest for precursory signals preceding earthquakes, radon monitoring has emerged as a research area experiencing continuous growth. Radon, a gas that emanates from the earth's interior to the surface, may be emitted during an earthquake. Anomalies in radon emissions from soil and hydrothermal systems have attracted significant attention as potentially useful earthquake precursors. Furthermore, this chapter aims to correlate the temporal decrease in b-value with the observed radon gas anomalies in various media.

6.2. Data Analysis

For the area bounded by latitudes 26° and 32° N and longitudes 80° and 90° E from 1900 to 2022, we compile an earthquake catalog from the ISC and the USGS consisting of 3888 events with Magnitude $M_W \geq 3.5$. In this investigation, we use the algorithm developed by [1] to locate and eliminate dependent events from the catalog. The technique is based on the assumption that the distribution of foreshocks and aftershocks in both space and time is influenced by the size of the primary event. For the [1] (as mentioned in Table 2.2 of chapter 2) declustering approach, we use the default parameters (tmin=1 day; tmax=10 days; XK= 0.5; Rfactor = 10 km) assigned in the Zmap [2] program to execute the declustering method. Various sources, including the ISC and USGS, contributed earthquake events to the compilation of the earthquake catalog, leading to the inclusion of events with different magnitude scales.

Sharma, V. and Biswas, R. Statistical analysis of seismic b-value using non-parametric Kolmogorov-Smirnov test and probabilistic seismic hazard parametrization for Nepal and its surrounding regions. Natural Hazards, 120: 7499–7526, 2024.

ISC and USGS utilize the M_D scale, the M_L scale, the mb scale, the M_S scale, and the M_W scale for magnitude measurement. To standardize the catalog, we must convert all events to a single magnitude scale. We use the equations suggested by [3] and [4] (as mentioned in Table 2.1 of chapter 2) to convert all earthquake catalog's magnitude scales to M_W.

6.3. Methodology

In this chapter, we employed the Aki-Utsu MLE [5], [6] for the determination of average b-value for the study area. Estimates of the SD, are obtained using the formula developed by [7].

6.4. Temporal anomalies in b-value and radon gas concentration

Figure 6.1 shows a temporal fluctuation in the b-value curve in the examined area, with a general tendency to decrease before the November 9, 2022 earthquake. [8] found an extremely low b-value in southwest China, possibly a precursor to the Wenchuan earthquake. The b-value slope had a negative gradient just before two significant earthquakes in Tokachi, Hokkaido, Japan, and September 26, 2003, and September 11, 2008, respectively [9]. [10] found a correlation between low b-values and mainshocks in the southern California area. Several studies suggest that fluctuation in the b-value at any seismic site can predict significant and moderate earthquakes. In a recent study, [11] used LR-115(II) solid state nuclear track detectors to observe the concentrations of radon and thorium in soil gas from July 15, 2011, to February 2, 2012, in order to analyze the soil concentrations of radon and thorium gas anomalies as an earthquake precursor. The results have been compared to the seismic activity that took place within 800 km of the measurement sites during the specified time period. The anomaly in radon gas concentrations observed in the Mat Bridge and Tuichang regions of Mizoram state is depicted in Figure 6.2. The devastating 2011 Nepal-Sikkim border earthquake (Mw 6.9) was reported in this period. [11] observed radon anomalies well before the occurrence of the 2011 Nepal-Sikkim earthquake. The increase in radon gas concentration was reported by [11] twenty days before the occurrence of the 2011 Nepal-Sikkim earthquake (Mw 6.8). Various studies (e.g., [12], [13], [14], [15]) have been carried out over the globe to analyse the radon gas anomaly as an earthquake precursor. Likewise, [16] reported a radon gas anomaly before the devastating (Ms = 8.1) Mexican earthquake of September 19, 1985. Previous research observed unusual increases in radon (222Rn) levels in soil, groundwater, and the atmosphere before major earthquakes. However, these studies often overlooked the influence of meteorological factors such as pressure, temperature, and rainfall. Thus, the recent studies consider all these factors while analyzing the anomalous characters of radon gas as an earthquake precursor. The different anomalous character was shown by ground water, soil and atmospheric before the occurrence of major earthquake. Likewise, the decrease in the concentration of atmospheric radon gas was reported by [17]. while, [18] reported fall in ground water radon gas concentration well before the occurrence of 2003 Chengkung earthquake (6.8), 2006 Taitung earthquake (6.1) and 2008 Autung earthquake (5.4). [19] found an unusual rise in soil radon concentration twenty-two days before an earthquake on Taal volcano, Luzon Island, the Philippines. A precursor phenomenon is one that takes place before to a mainshock and serves as physical foreplay for the main rupture. Many writers have regularly studied earthquake precursor phenomena. Likewise, Systematic research has been done to determine if temporal variations in b-value may serve as a short-, medium-, and long-term earthquake precursor. The findings indicate that major earthquakes often have a medium-term rise in b, which is followed by a fall in the weeks and months before the earthquake [20]. Foreshocks that occur hours to days before the mainshock were the subject of a study by [21]. The b-value of foreshocks decreases by around 50%, according to research by [22] using both regional and worldwide earthquake databases. Using seismic data for Central America from PDE and Ecatalogs, [23] found that the b-value drops by a large amount before big earthquakes. In the present study the temporal variation observed in the b-value is analyzed for the study region. It can be inferred from the Figure 6.1 that the temporal curve shows decline well before the occurrence of major events including the 2011 Nepal-Sikkim earthquake (M_W 6.8), 2015 Gorkha earthquake (M_W 7.8) and 2022 Nepal earthquake (M_W 6.3). Various studies (including [24], [8], [9], [25]) have been carried to analyze the temporal variation of b-value before the occurrence of major events. These studies inferred that a significant fall in b-value is observed well before the occurrence of these major events. Thus, the general trend of fall in b-value before the occurrence of any Major events are reported by all the earlier studies. Due to multiple application of b-value in seismic hazard studies. Many researchers established its plausible correlation with other parameters including Seismic moment, focal depth, Stress, fractal Dimension, Bouguer gravity anomaly etc. In this chapter an attempt has been made to establish a plausible relationship between soil radon concentration, ground water gas anomaly and atmospheric radon anomaly. The comparative analysis of temporal b-value and radon gas anomaly inferred an antithetical relation between b-value and soil radon gas anomaly. The region reported with fall in b-value may be characterized increase in soil radon gas concentration and vice-versa. Meanwhile Positive correlation between temporal variation of b-value and ground water, Atmospheric radon gas anomaly is inferred from the present study. The regions reported with fall in b-values are characterized by the decrease in atmospheric and ground water radon gas anomaly.

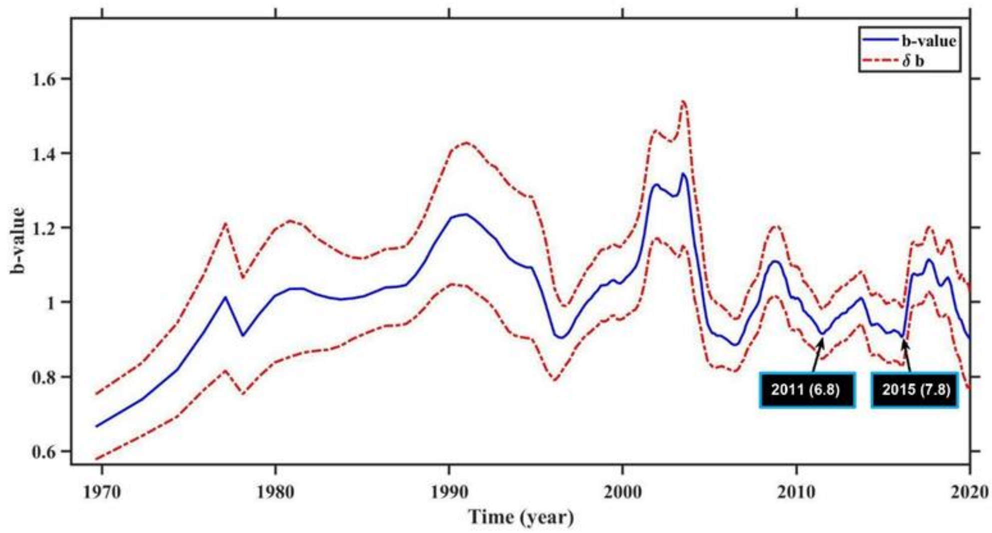

Figure 6.1. The temporal variation curve of b-value for the study region. The fall in b-value before 2011 (6.8) and 2015 (7.8) is illustrated in the figure.

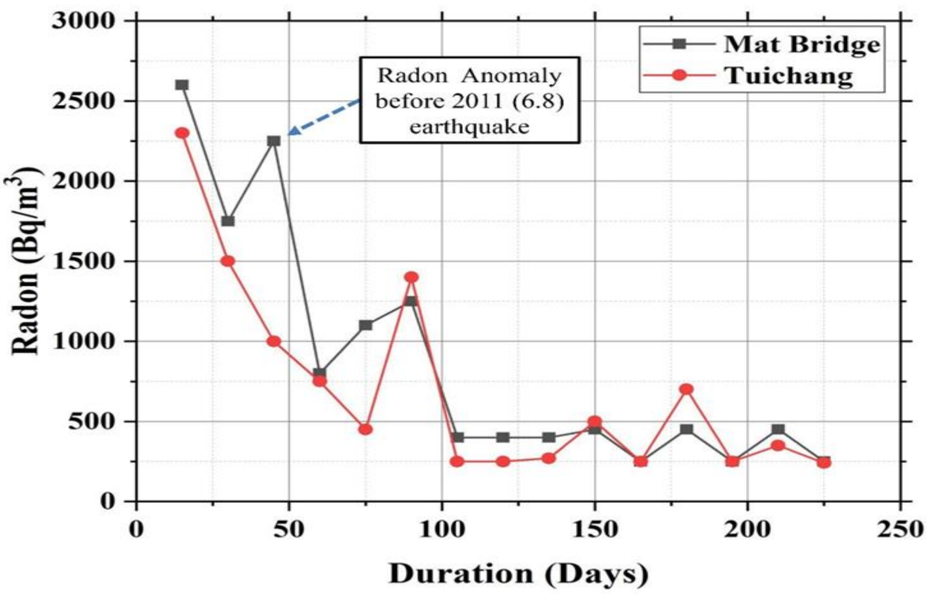

Figure 6.2. The Radon concentration (Bq/m3) observed at Mat Bride and Tuichang, Serchhip district, Mizoram observed between July 2011 to February 2012.

6.5. References

[1] Reasenberg, P. Second-order moment of central California seismicity 1969–1982. *Journal of Geophysical Research: Solid Earth,* 90(B7): 5479–5495, 1985.

[2] Wiemer, S. A software package to analyze seismicity: Zmap. *Seismological Research Letters,* 72(3): 373–382, 2001.

[3] Nath, S.K., Mandal, S., Das Adhikari, M. and Maiti, S.K. Unified earthquake catalogue for South Asia covering the period: 1900–2014. *Natural Hazards,* 85(3): 1787–1810, 2017.

[4] Kolathayar, S., Sitharam, T. G. and Vipin, K. S. Spatial variation of seismicity parameters across India and adjoining areas. *Natural Hazards,* 60(3): 1365–1379, 2012.

[5] Aki, K. Maximum likelihood estimate of b in the formula log N= a-bm and its confidence limits. *Bulletin of Earthquake Research Institute,* 43: 237–239, 1965.

[6] Utsu, T. A method for determining the value of the formula log N = a - bM showing the magnitude-frequency relation for earthquakes. *Geophysical bulletin of Hokkaido University,* 13: 99–103, 1965.

[7] Shi, Y. and Bolt, B. A. The standard error of the magnitude-frequency b value. *Bulletin of the Seismological Society of America,* 72(5): 1677–1687, 1982.

[8] Zhang, S. and Zhou, S. Spatial and temporal variation of B-values in Southwest China. *Pure and Applied Geophysics,* 173(1): 85–96, 2016.

[9] Xie, W., Hattori, K. and Han, P. Temporal variation and statistical assessment of the b value off the pacific coast of Tokachi, Hokkaido, Japan. *Entropy,* 21(3): 2019.

[10] Henderson, J. R., Main, I. G., Pearce, R. G. and Takeya, M. K. Seismicity in North-Eastern Brazil—fractal clustering and the evolution of the b-value. *Geophysical Journal International,* 116(1): 217–226, 1994.

[11] Jaishi, H. P., Singh, S., Tiwari, R. P. and Tiwari, R. C. Radon and thoron anomalies along Mat fault in Mizoram, India. *Journal of Earth System Science,* 122(6): 1507–1513, 2013.

[12] Ghosh, D., Deb, A. and Sengupta, R. Anomalous radon emission as precursor of earthquake. *Journal of Applied Geophysics,* 69(2): 67–81, 2009.

[13] Chowdhury, S., Deb, A., Barman, C., Nurujjaman, M. and Bora, D. K. Simultaneous monitoring of soil 222Rn in the Eastern Himalayas and the geothermal region of eastern India: An earthquake precursor. *Natural Hazards,* 112(2): 1477–1502, 2022.

[14] Jin, X., Bu, J., Qiu, G., Ma, L., Chen, Z., Chen, T., Wu, J., Pan, B., Ji, H., Tian, J., Wu, X., Li, Z., Zhang, L., Liu, C., Zhao, X. and Cheng, X. Non-normal distribution of radon and residual radon and short-term abnormal precursors of residual radon before major earthquakes. *Earth Science Informatics,* 15(4): 2495–2511, 2022.

[15] Bose, A. G., Das, A., Chowdhury, S. and Deb, A. Studies of scintillations and TEC variations with GPS satellite links together with soil radon anomalies preceding Nepal earthquakes of April–May 2015. *Natural Hazards,* 112(2): 1137–1163, 2022.

[16] Segovia, N., de la Cruz-Reyna, S., Mena, M., Ramos, E., Monnin, M. and Seidel, J. L. Radon in soil anomaly observed at Los Azufres geothermal field, Michoacan: a possible precursor of the 1985 Mexico earthquake (Ms = 8.1). *Natural Hazards,* 1(4): 319–329, 1989.

[17] Muto, J., Yasuoka, Y., Miura, N., Iwata, D., Nagahama, H., Hirano, M., Ohmomo, Y. and Mukai, T. Preseismic atmospheric radon anomaly associated with 2018 Northern Osaka earthquake. *Scientific Reports,* 11(1): 7451, 2021.

[18] Kuo, T., Su, C., Chang, C., Lin, C., Cheng, W., Liang, H., Lewis, C. and Chiang, C. Application of recurrent radon precursors for forecasting large earthquakes (Mw > 6.0) near Antung, Taiwan. *Radiation Measurements,* 45(9): 1049–1054, 2010.

[19] Richon, P., Klinger, Y., Tapponnier, P., Li, C. X., Van Der Woerd, J. and Perrier, F. Measuring radon flux across active faults: Relevance of excavating and possibility of satellite discharges. *Radiation Measurements,* 45(2): 211–218, 2010.

[20] Sammonds, P. R., Meredith, P. G. and Main, I. G. Role of pore fluids in the generation of seismic precursors to shear fracture. *Nature,* 359(6392): 228–230, 1992.

[21] Molchan, G. M. and Dmitrieva, O. E. Dynamics of the magnitude—frequency relation for foreshocks. *Physics of the Earth and Planetary Interiors,* 61(1–2): 99–112, 1990.

[22] Molchan, G. M., Kronrod, T. L. and Nekrasova, A. K. Immediate foreshocks: Time variation of the b-value. *Physics of the Earth and Planetary Interiors,* 111(3–4): 229–240, 1999.

[23] Monterroso Juárez, D. A. Statistical seismology studies in Central America: b-value, seismic hazard and seismic quiescence. *Acta Universitatis Upsaliensis,* 2003.

[24] Nuannin, P., Kulhanek, O. and Persson, L. Spatial and temporal b value anomalies preceding the devastating off coast of NW Sumatra earthquake of December 26, 2004. *Geophysical Research Letters,* 32(11): 2005.

[25] Xie, Z., Lyu, Y. and Li, X. Temporal and spatial changes in the b-value prior to the 2021 Luxian MS 6.0 earthquake in Sichuan, China. *Geomatics, Natural Hazards and Risk,* 13(1): 934–948, 2022.